VIP Electrochemistry Very Important Paper

International Edition: DOI: 10.1002/anie.201711552
German Edition: DOI: 10.1002/ange.201711552

Ion–Solvent Complexes Promote Gas Evolution from Electrolytes on a Sodium Metal Anode

*Xiang Chen, Xin Shen, Bo Li, Hong-Jie Peng, Xin-Bing Cheng, Bo-Quan Li, Xue-Qiang Zhang, Jia-Qi Huang, and Qiang Zhang**

Abstract: *Lithium and sodium metal batteries are considered as promising next-generation energy storage devices due to their ultrahigh energy densities. The high reactivity of alkali metal toward organic solvents and salts results in side reactions, which further lead to undesirable electrolyte depletion, cell failure, and evolution of flammable gas. Herein, first-principles calculations and in situ optical microscopy are used to study the mechanism of organic electrolyte decomposition and gas evolution on a sodium metal anode. Once complexed with sodium ions, solvent molecules show a reduced LUMO, which facilitates the electrolyte decomposition and gas evolution. Such a general mechanism is also applicable to lithium and other metal anodes. We uncover the critical role of ion–solvent complexation for the stability of alkali metal anodes, reveal the mechanism of electrolyte gassing, and provide a mechanistic guidance to electrolyte and lithium/sodium anode design for safe rechargeable batteries.*

Batteries, one of the major power sources in daily society life, have nowadays become an indispensable technology.[1] Particularly, alkali metal batteries are considered as one of the most promising next-generation energy storage devices owing to their high energy densities.[2] For instance, Li metal batteries (LMBs), employing a Li metal anode and a high-capacity cathode such as oxygen and sulfur, consequently deliver a high specific energy (non-aqueous Li–oxygen battery: 3505 $Wh\,kg^{-1}$; Li–sulfur battery: 2600 $Wh\,kg^{-1}$). Sodium, having a theoretical specific capacity of 1160 $mAh\,g^{-1}$, is expected to be a more abundant, cost-effective and sustainable alternative to Li as anode material for high-energy-density batteries adopting an oxygen or sulfur cathode.[3,4] Therefore, Na metal batteries (SMBs) are expected to achieve great success in the field of large-scale and low-cost energy storage.[5]

However, the practicality of Na metal anodes for rechargeable SMBs is facing tremendous challenges. The Na metal anode is much more reactive than a routine carbonaceous anode based on ion intercalation chemistry. The high reactivity is the origin of uncontrollable side reactions and electrolyte depletion.[6] The continuous consumption of both Na and electrolyte leads to a low Coulombic efficiency and short life cycle. More importantly, most organic electrolytes are easily reduced on Na, generating flammable gases. The exothermic nature of the above reduction reactions, combined with flammable gas evolution, induces severe safety hazards.[7]

The imperative for a practical and safe SMB is to understand the chemistry of the Na/electrolyte interplay and the mechanism of gas evolution. Currently, most efforts mainly focus on materials and structure design for stable Na anodes. Luo and co-workers employed porous aluminum as a Na host, achieving a dendrite-free Na anode with a high average Coulombic efficiency above 99.9% during 1000 cycles. Pint and colleagues described an in situ plated Na anode through the use of a nanocarbon nucleation layer on aluminum current collectors, which enabled dendrite-free and highly reversible deposition.[4] Despite the success of the above-menioned nanostructured hosts in regulating the stripping/plating of Na metal,[8] it is challenging to realize a safe SMB due to the lack of both strategies for interface stabilization and the understanding of electrolyte gassing in the presence of Na.[9,10]

Herein, gas evolution from organic electrolytes on a Na metal anode is understood through first-principles calculations and in situ optical microscopic observations. Propylene carbonate (PC), one of the common solvents, is selected as the major research target. According to in situ optical microscopic observations, a PC solution containing 1.0 M sodium perchlorate ($NaClO_4$) salt (referred to Na^+–PC solution) was first probed to decompose more violently than pure PC solvent. To unveil such a unique phenomenon, first-principles calculations suggest that it is the ion–solvent complex ($[NaPC]^+$), which possesses a lower level of LUMO (the lowest unoccupied molecular orbital) than that of pure PC solvent, to be more easily reduced on Na, triggering gas evolution. The *ab initio* molecular dynamics (AIMD) simulations revealed the kinetic behavior of electrolyte gassing on

[*] X. Chen, X. Shen, H.-J. Peng, Dr. X.-B. Cheng, B.-Q. Li, X.-Q. Zhang, Prof. Q. Zhang
Beijing Key Laboratory of Green Chemical Reaction Engineering and Technology
Department of Chemical Engineering
Tsinghua University, Beijing 100084 (P. R. China)
E-mail: zhang-qiang@mails.tsinghua.edu.cn
Prof. B. Li
Shenyang National Laboratory for Materials Science
Institute of Metal Research, Chinese Academy of Sciences
72 Wenhua Road, Shenyang 110016 (P. R. China)
Prof. J.-Q. Huang
Advanced Research Institute of Multidisciplinary Science
Beijing Institute of Technology
Beijing 100081 (P. R. China)
Prof. Q. Zhang
Key Laboratory of Advanced Energy Materials Chemistry (Ministry of Education), Nankai University
Tianjin 300071 (P. R. China)
Supporting information and the ORCID identification number(s) for the author(s) of this article can be found under: https://doi.org/10.1002/anie.201711552.

Na. The observations and understanding were shown in other electrolyte systems with solvents ranging from carbonates to ethers (see Figure S1 in the Supporting Information), as well as in studies of Li/electrolyte interplay, exhibiting general and mechanistic insights.

In situ optical microscopy is a useful tool to visualize macroscopic phenomena like gas bubbling and dendrite growth. Figure 1, as well as movies S1 and S2, depicts

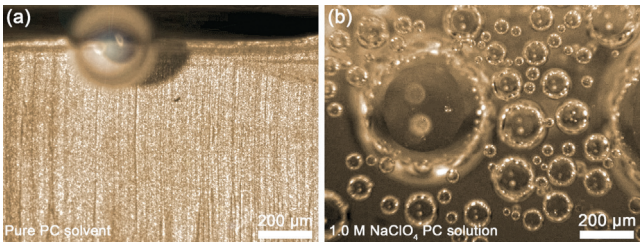

Figure 1. In situ optical microscopic images of gas evolution on Na: a) pure PC solvent. b) Na^+–PC solution. The images are captured from movies S1 and S2.

distinguished gassing behavior of pure PC solvent and Na^+–PC solution in contact with Na. Both PC solvent and Na^+–PC solution suffer from spontaneous side reactions once being in contact with Na, which indicates the unstable Na/electrolyte interface. However, the gassing rate of Na^+–PC solution is almost ten times higher than that of PC solvent. Such a difference in gassing rate can only be ascribed to the presence of ions. Thus, it is hypothesized that the ion–solvent complex $[NaPC]^+$, of which the role in reactions on Na and other alkali metals has rarely been disclosed, is responsible for the enhanced gas evolution.

To unveil the distinguished chemistry of $[NaPC]^+$ from PC, frontier molecular orbital analysis was conducted by first-principles calculations. Herein, the LUMO level of PC is −0.60 eV (Figure 2a). Considering the solvent effects through an integral equation formalism variant of the polarizable continuum (IEFPCM) model,[11] the LUMO level of PC was calculated to be −0.17 eV. This shows the benefits of solvent effects in enhancing the chemical stability of solvents toward Na. Once a PC molecule is complexed with a Na^+ ion, the LUMO level of the corresponding $[NaPC]^+$ complex sharply decreases to −5.28 eV, indicating that the $[NaPC]^+$ complex is much easier to be reduced. The huge difference in energetics between PC and $[NaPC]^+$, as large as 5.11 eV, explains the above hypothesis raised during in situ observations that ion complexation weakens the stability of solvent molecule and thus promotes the gassing reactions.

Further orbital analysis of $[NaPC]^+$ and another neutral complex of a PC molecule with a Na atom (referred to [NaPC]) was performed to explain the lowering mechanism of LUMO levels of $[NaPC]^+$ and [NaPC]. When a PC molecule interacts with a Na^+ ion, the HOMO of PC and the LUMO of the Na^+ ion are hybridized and they rearrange into two new hybrid orbitals (Figure 2b). Similarly, the HOMO of PC and SOMO (singly occupied molecular orbital) of the Na atom can be hybridized (Figure 2c). The lowered LUMO levels of

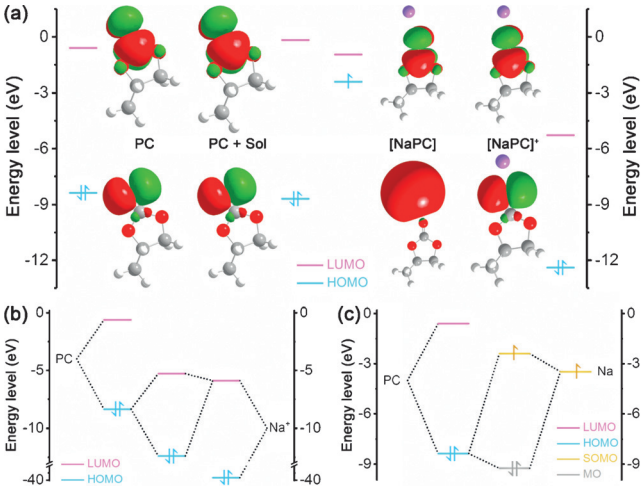

Figure 2. Frontier molecular orbital theory analysis. a) Frontier molecular orbital levels of PC (single PC molecule), PC + Sol (PC molecule with solvent effects considered), [NaPC] (Na-atom–PC complex) and $[NaPC]^+$ (Na^+-ion–PC complex). The red and green regions represent the positive and negative parts of the LUMO and HOMO wave functions, respectively (isovalue: 0.02). The hydrogen, lithium, carbon, and oxygen atoms are marked with white, purple, gray, and red, respectively. Schematics for the orbital hybridization between PC and b) Na^+ ion and c) Na atom.

the $[NaPC]^+$ and [NaPC] complexes are thereby ascribed to the orbital hybridization.

Aside from thermodynamic energetics, the kinetics of electrolyte gassing on Na is also important. AIMD simulations were thereafter conducted. Two reaction mechanisms of electrolyte decomposition were proposed (Figure 3 and Figure S2, movie S3). In the first mechanism, a PC molecule is reduced to form a carbon monoxide and an organic Na salt (Figure 3a–c and Figure S2a). According to the bond length

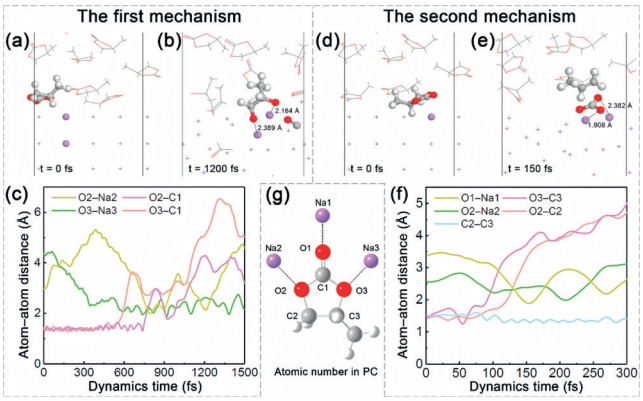

Figure 3. AIMD simulations of the decomposition of PC on Na (110) surface. First decomposition mechanism: a) the initial state of the PC molecule; b) the decomposed PC at 1200 fs; c) time evolution of the whole decomposition process. Second decomposition mechanism: d) the initial state of the PC molecule; e) the decomposed PC at 150 fs; f) time evolution of the whole decomposition process; g) atomic number of PC used in (c) and (f). The hydrogen, lithium, carbon, and oxygen atoms are marked with white, purple, gray, and red, respectively. Only the reacted PC and Na are present with ball-and-stick model. The other atoms are present with lines.

analysis, the O3 atom of PC is first bonded to the Na^+ ion (Na3), accompanied by an electron transferring from the C1 to O3 atom of PC. As a result, the C1–O3 bond breaks at around 570 fs during the AIMD simulation. Afterward, the O2 atom donates an electron to the C1 atom due to a strong electron-withdrawing effect of the carbenium ion, rendering the C1–O2 bond to break and release a carbon monoxide molecule after around 187 fs. Finally, the as-obtained intermediate is bonded to another Na^+ ion (Na2) and accepts two electrons from Na metal, giving an organic Na salt as the final product.

In the second mechanism, propene and sodium carbonate are the products of the reaction (Figure 3 d–f and Figure S2b). Unlike the first mechanism, the O1 atom is the first oxygen atom that coordinates with the Na^+ ion. Similarly, this step is also accompanied by an electron transfer from C1 to O1. Driven by a strong electron-withdrawing effect, the electron transfers sequentially from C3 to O3, and to C1, resulting in C3–O3 bond breaking at around 70 fs during the AIMD simulation. After 39 fs, another electron is donated from O2 to C2, and to C3 as compensation. The C2–O2 bond consequently breaks and the O2 accepts a Na^+ ion and two electrons, finally resulting in a propene and a sodium carbonate. Besides, the bond length of C2–C3 is reduced from 1.52 to 1.35 Å, suggesting the transition from a C–C bond in PC to a C=C bond in propene.

The two proposed mechanisms share the following common characters: 1) a solvated Na^+ ion is necessary to break the C–O bond, highlighting the role of the $[NaPC]^+$ complex; 2) the C–O bonds (C1–O3 and C3–O3) near the methyl are the first breaking bonds since the electron-donating methyl group enriches the electron density of the oxygen atom to attract the Na^+ ion more easily than other oxygen atoms; 3) it is relatively easy to break the second C–O bond compared to the first one, which has also been reported for 1,2-dimethoxyethane (DME) and 1,3-dioxolane (DOL) solvent in the presence of Li;[12] 4) flammable gases, that is, carbon monoxide and propene, are the final products, increasing the safety hazards.

The generality of the above-demonstrated mechanism for promoted gas evolution on Na by ion–solvent complexes was further validated on other solvent systems, such as DME and tetraethylene glycol dimethyl ether (TEGDME). DME and TEGDME are two typical ether solvents that are frequently used in SMBs because of their better stability relative to that of carbonates. Similar to the case of PC, Na^+–DME and TEMDME solutions suffer from an enhanced gas evolution on Na relative to pure DME and TEGDME solvents as observed by in situ optical microscopy (Figure S3 and movies S4–S7). Further quantum chemical calculations validate that the LUMO levels of both $[NaDME]^+$ and $[NaTEGDME]^+$ complexes are much lower than that of pure DME and TEGDME solvents, respectively (Figures S4 and S5, Table S1). All above-mentioned results resemble the same scheme of an ion–solvent complex that possesses poorer thermodynamic stability than its non-ion-coordinated counterpart and therefore, the ion-containing electrolyte exhibits a higher gas-evolving rate than the pure solvent when being in contact with Na.

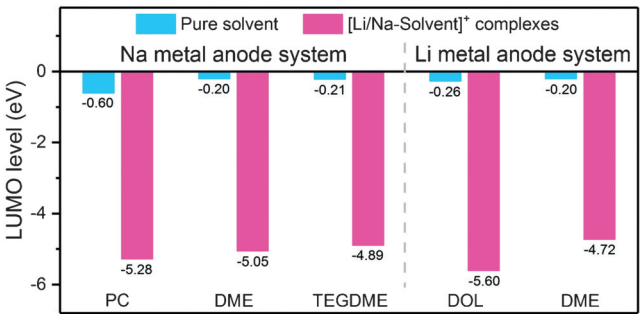

Figure 4. Comparisons among the LUMO levels of pure solvents and ion–solvent complexes in Na and Li metal anode systems.

Replacing the Na by Li does not change the general mechanism. Two typical solvents used in LMBs, DOL and DME, are considered herein. According to first-principles calculations, the LUMO levels of $[LiDOL]^+$ and $[LiDME]^+$ complexes are decreased by 5.34 and 4.52 eV compared to that of pure DOL and DME solvents, respectively, implying the Li^+–solvent complexes are more reactive toward Li than the pure solvents (Figure 4).[12] In situ optical microscopy was also used to visualize the theoretical prediction. Gas evolution from Li^+–DOL and DME solutions was more vigorous on Li than in pure solvents (movies S8–S11). The Li salt herein has a anion, bi(trifluoromethanesulfonyl)imidate ($TFSI^-$), different from that of the Na salt, that is, ClO_4^-. The similar phenomena observed on Na and Li suggest that the cation coordination, instead of anion, plays a dominant role in the electrolyte decomposition and gas evolution. Such a general mechanism is believed to be applicable to other metal anodes especially alkali and alkaline earth metals (potassium, cesium, magnesium, calcium, etc.).[13]

The new insight into ion–solvent complexes is of both fundamental significance to the understanding of the electrolyte gassing mechanism and practical guidance to electrolyte screening and metal anode design. First, the redox potentials of organic solvent are usually employed as descriptors of electrolyte stability. This study indicates that the redox potentials of the ion–solvent complexes exhibit higher values as parameters for electrolyte screening. Besides, the scaling relationship between pure solvents and corresponding ion–solvent complexes is worth investigations. Second, this understanding inspires us to propose a possible strategy to stabilize ion (e.g., A^{x+})–solvent complexes by introducing a different cation (e.g., B^{y+}) that is more easily coordinated by the solvent but chemically more inert than A^{x+}. Besides, recent advances in high-salt-concentration electrolytes show the great potential of conducting deep theoretical studies on more complicated ion–solvent structures such as dimers and clusters, which are always found at high salt concentration.[14] The difference in local ion–solvent structures is believed to give new insights. These future insights are expected to revolutionize current electrolyte recipes.[15] Third, since most of the organic solvents are intrinsically reducible by Li and Na while ion–solvent complexes ubiquitously exist in any known electrolyte system, designing an artificial or in situ protective layer on the alkali metal anode to prevent its direct contact to unstable ion–solvent complexes emerges as a more promising

and feasible approach to suppress undesirable gas evolution than searching for a "stable" solvent.[9,16]

In conclusion, the concept of ion–solvent complexes promoting gas evolution from electrolytes on alkali metal anodes is theoretically and experimentally verified. Ion-containing solutions suffer from much more violent gas evolution on Na than in pure solvents, which is attributed to the lower LUMO level of the ion–solvent complex than that of the corresponding solvent. The gassing reaction mechanism was further illustrated through AIMD simulations. The general principle is applicable to various electrolyte (e.g., PC, DME, TEGDME, and DOL)–metal (e.g., Na and Li) systems. This work uncovers the important role of ion–solvent complexes and reveals the nature of electrolyte gassing, rendering mechanistic insights to advanced electrolyte screening and rational design of Li/Na metal anodes for safe rechargeable batteries.

Acknowledgements

This work was supported by National Key Research and Development Program (grant numbers 2016YFA0202500 and 2016YFA0200102), and National Natural Scientific Foundation of China (grant number 21676160). The calculations were supported by Tsinghua National Laboratory for Information Science and Technology. We thank Chen-Zi Zhao and Rui Zhang for helpful discussion.

Conflict of interest

The authors declare no conflict of interest.

Keywords: electrochemistry · electrolytes · first-principles calculations · gas evolution · alkali metal batteries

How to cite: *Angew. Chem. Int. Ed.* **2018**, *57*, 734–737
Angew. Chem. **2018**, *130*, 742–745

[1] M. Armand, J. M. Tarascon, *Nature* **2008**, *451*, 652–657; N. S. Choi, Z. Chen, S. A. Freunberger, X. Ji, Y. K. Sun, K. Amine, G. Yushin, L. F. Nazar, J. Cho, P. G. Bruce, *Angew. Chem. Int. Ed.* **2012**, *51*, 9994–10024; *Angew. Chem.* **2012**, *124*, 10134–10166; J. W. Choi, D. Aurbach, *Nat. Rev. Mater.* **2016**, *1*, 16013.

[2] H. J. Peng, J. Q. Huang, Q. Zhang, *Chem. Soc. Rev.* **2017**, *46*, 5237–5288; X. B. Cheng, R. Zhang, C. Z. Zhao, Q. Zhang, *Chem. Rev.* **2017**, *117*, 10403–10473; R. Zhang, N. W. Li, X. B. Cheng, Y. X. Yin, Q. Zhang, Y. G. Guo, *Adv. Sci.* **2017**, *4*, 1600445; G. Zhang, Z. W. Zhang, H. J. Peng, J. Q. Huang, Q. Zhang, *Small Methods* **2017**, *1*, 1700134; H. J. Peng, J. Q. Huang, X. B. Cheng, Q. Zhang, *Adv. Energy Mater.* **2017**, *7*, 1700260.

[3] M. D. Slater, D. Kim, E. Lee, C. S. Johnson, *Adv. Funct. Mater.* **2013**, *23*, 947–958; D. Larcher, J. M. Tarascon, *Nat. Chem.* **2015**, *7*, 19–29; L. P. Wang, L. H. Yu, X. Wang, M. Srinivasan, Z. C. J. Xu, *J. Mater. Chem. A* **2015**, *3*, 9353–9378; J. Brückner, S. Thieme, H. T. Grossmann, S. Dörfler, H. Althues, S. Kaskel, *J. Power Sources* **2014**, *268*, 82–87.

[4] A. P. Cohn, N. Muralidharan, R. Carter, K. Share, C. L. Pint, *Nano Lett.* **2017**, *17*, 1296–1301.

[5] Y. X. Wang, B. Zhang, W. Lai, Y. Xu, S. L. Chou, H. K. Liu, S. X. Dou, *Adv. Energy Mater.* **2017**, *7*, 1602829; K. Song, D. A. Agyeman, M. Park, J. Yang, Y. M. Kang, *Adv. Mater.* **2017**, *29*, 1606572; D. Ruiz-Martinez, A. Kovacs, R. Gomez, *Energy Environ. Sci.* **2017**, *10*, 1936–1941.

[6] A. Wang, X. Hu, H. Tang, C. Zhang, S. Liu, Y. W. Yang, Q. H. Yang, J. Luo, *Angew. Chem. Int. Ed.* **2017**, *56*, 11921–11926; *Angew. Chem.* **2017**, *129*, 12083–12088.

[7] R. Rodriguez, K. E. Loeffler, S. S. Nathan, J. K. Sheavly, A. Dolocan, A. Heller, C. B. Mullins, *ACS Energy Lett.* **2017**, *2*, 2051–2057.

[8] W. Luo, Y. Zhang, S. Xu, J. Dai, E. Hitz, Y. Li, C. Yang, C. Chen, B. Liu, L. Hu, *Nano Lett.* **2017**, *17*, 3792–3797; H. J. Yoon, N. R. Kim, H. J. Jin, Y. S. Yun, *Adv. Energy Mater.* **2017**, *7*, 1701261; Y. Lu, Q. Zhang, M. Han, J. Chen, *Chem. Commun.* **2017**, DOI: https://doi.org/10.1039/C7CC07485A; J. Gu, Z. Du, C. Zhang, J. Ma, B. Li, S. Yang, *Adv. Energy Mater.* **2017**, *7*, 1700447.

[9] W. Luo, C. F. Lin, O. Zhao, M. Noked, Y. Zhang, G. W. Rubloff, L. B. Hu, *Adv. Energy Mater.* **2017**, *7*, 1601526.

[10] Z. W. Seh, J. Sun, Y. Sun, Y. Cui, *ACS Cent. Sci.* **2015**, *1*, 449–455.

[11] B. Mennucci, *Wiley Interdiscip. Rev.: Comput. Mol. Sci.* **2012**, *2*, 386–404.

[12] X. Chen, T. Z. Hou, B. Li, C. Yan, L. Zhu, C. Guan, X. B. Cheng, H. J. Peng, J. Q. Huang, Q. Zhang, *Energy Storage Mater.* **2017**, *8*, 194–201.

[13] H. M. Kwon, M. L. Thomas, R. Tatara, Y. Oda, Y. Kobayashi, A. Nakanishi, K. Ueno, K. Dokko, M. Watanabe, *ACS Appl. Mater. Interfaces* **2017**, *9*, 6014–6021; K. Yoshida, M. Nakamura, Y. Kazue, N. Tachikawa, S. Tsuzuki, S. Seki, K. Dokko, M. Watanabe, *J. Am. Chem. Soc.* **2011**, *133*, 13121–13129; S. Tsuzuki, T. Mandai, S. Suzuki, W. Shinoda, T. Nakamura, T. Morishita, K. Ueno, S. Seki, Y. Umebayashi, K. Dokko, M. Watanabe, *Phys. Chem. Chem. Phys.* **2017**, *19*, 18262–18272.

[14] J. Qian, W. A. Henderson, W. Xu, P. Bhattacharya, M. Engelhard, O. Borodin, J. G. Zhang, *Nat. Commun.* **2015**, *6*, 6362.

[15] X. Q. Zhang, X. B. Cheng, X. Chen, C. Yan, Q. Zhang, *Adv. Funct. Mater.* **2017**, *27*, 1605989; H. Yu, J. Zhao, L. Ben, Y. Zhan, Y. Wu, X. Huang, *ACS Energy Lett.* **2017**, *2*, 1296–1302; Y. Zhang, J. Qian, W. Xu, S. M. Russell, X. Chen, E. Nasybulin, P. Bhattacharya, M. H. Engelhard, D. Mei, R. Cao, F. Ding, A. V. Cresce, K. Xu, J. G. Zhang, *Nano Lett.* **2014**, *14*, 6889–6896; L. Cheng, L. A. Curtiss, K. R. Zavadil, A. A. Gewirth, Y. Shao, K. G. Gallagher, *ACS Energy Lett.* **2016**, *1*, 503–509.

[16] Y. Zhao, L. V. Goncharova, Q. Zhang, P. Kaghazchi, Q. Sun, A. Lushington, B. Wang, R. Li, X. Sun, *Nano Lett.* **2017**, *17*, 5653–5659; Y. Zhao, L. V. Goncharova, A. Lushington, Q. Sun, H. Yadegari, B. Wang, W. Xiao, R. Li, X. Sun, *Adv. Mater.* **2017**, *29*, 1606663; X. B. Cheng, C. Yan, X. Chen, C. Guan, J. Q. Huang, H. J. Peng, R. Zhang, S. T. Yang, Q. Zhang, *Chem* **2017**, *2*, 258–270; C. Z. Zhao, X. B. Cheng, R. Zhang, H. J. Peng, J. Q. Huang, R. Ran, Z. H. Huang, F. Wei, Q. Zhang, *Energy Storage Mater.* **2016**, *3*, 77–84; S. Choudhury, S. Wei, Y. Ozhabes, D. Gunceler, M. J. Zachman, Z. Tu, J. H. Shin, P. Nath, A. Agrawal, L. F. Kourkoutis, T. A. Arias, L. A. Archer, *Nat. Commun.* **2017**, *8*, 898; H. Wang, C. Wang, E. Matios, W. Li, *Nano Lett.* **2017**, *17*, 6808–6815; H. Tian, Z. W. Seh, K. Yan, Z. Fu, P. Tang, Y. Lu, R. Zhang, D. Legut, Y. Cui, Q. Zhang, *Adv. Energy Mater.* **2017**, *7*, 1602528; B. Li, D. Zhang, Y. Liu, Y. Yu, S. Li, S. Yang, *Nano Energy* **2017**, *39*, 654–661.

Manuscript received: November 10, 2017
Accepted manuscript online: November 27, 2017
Version of record online: December 12, 2017

